Title
Maintenance of Tight Junction Integrity in the Absence of Vascular Dilation in the Brain of Mice Exposed to Ultra-High-Dose-Rate FLASH Irradiation

Journal
Radiation Research, 194(6)

ISSN
0033-7587

Authors
Allen, Barrett D
Acharya, Munjal M
Montay-Gruel, Pierre
et al.

Publication Date
2020-12-01

DOI
10.1667/rade-20-00060.1

Peer reviewed

HHS Public Access

Author manuscript

Radiat Res. Author manuscript; available in PMC 2020 December 30.

Published in final edited form as:

Radiat Res. 2020 December 01; 194(6): 625–635. doi:10.1667/RADE-20-00060.1.

Maintenance of Tight Junction Integrity in the Absence of Vascular Dilation in the Brain of Mice Exposed to Ultra-High-Dose-Rate FLASH Irradiation

Barrett D. Allen[a], **Munjal M. Acharya**[a], **Pierre Montay-Gruel**[b], **Patrik Goncalves Jorge**[b,c], **Claude Bailat**[c], **Benoît Petit**[b], **Marie-Catherine Vozenin**[b,1], **Charles Limoli**[a,1]

[a]Department of Radiation Oncology, University of California, Irvine, Irvine, California 92697-2695; [b]Laboratory of Radiation Oncology, Department of Radiation Oncology, Lausanne University Hospital and University of Lausanne, Lausanne, Switzerland; [c]Institute of Radiation Physics/CHUV, Lausanne University Hospital, Lausanne, Switzerland

Abstract

Persistent vasculature abnormalities contribute to an altered CNS microenvironment that further compromises the integrity of the blood-brain barrier and exposes the brain to a host of neurotoxic conditions. Standard radiation therapy at conventional (CONV) dose rate elicits short-term damage to the blood-brain barrier by disrupting supportive cells, vasculature volume and tight junction proteins. While current clinical applications of cranial radiotherapy use dose fractionation to reduce normal tissue damage, these treatments still cause significant complications. While dose escalation enhances treatment of radiation-resistant tumors, methods to subvert normal tissue damage are clearly needed. In this regard, we have recently developed a new modality of irradiation based on the use of ultra-high-dose-rate FLASH that does not induce the classical pathogenic patterns caused by CONV irradiation. In previous work, we optimized the physical parameters required to minimize normal brain toxicity (i.e., FLASH, instantaneous intra-pulse dose rate, $6.9 \cdot 10^6$ Gy/s, at a mean dose rate of 2,500 Gy/s), which we then used in the current study to determine the effect of FLASH on the integrity of the vasculature and the blood-brain barrier. Both early (24 h, one week) and late (one month) timepoints postirradiation were investigated using C57Bl/6J female mice exposed to whole-brain irradiation delivered in single doses of 25 Gy and 10 Gy, respectively, using CONV (0.09 Gy/s) or FLASH (>10^6 Gy/s). While the majority of changes found one day postirradiation were minimal, FLASH was found to reduce levels of apoptosis in the neurogenic regions of the brain at this time. At one week and one month postirradiation, CONV was found to induce vascular dilation, a well described sign of vascular alteration, while FLASH minimized these effects. These results were positively correlated with and temporally coincident to changes in the immunostaining of the vasodilator eNOS colocalized to the vasculature, suggestive of possible dysregulation in blood flow at these latter times. Overall expression of the tight junction proteins, occludin and claudin-5, which was significantly reduced after CONV irradiation, remained unchanged in the FLASH-irradiated brains at one and four

[1]Address for correspondence: Laboratoire de Radio-Oncologie, Centre Hospitalier, Universitaire Vaudois, Bugnon 46, 1011 Lausanne, Switzerland; Marie-Catherine.Vozenin@chuv.ch or Department of Radiation Oncology, University of California, Irvine, Irvine, CA 92617-2695; climoli@uci.edu.

weeks postirradiation. Our data further confirm that, compared to isodoses of CONV irradiation known to elicit detrimental effects, FLASH does not damage the normal vasculature. These data now provide the first evidence that FLASH preserves microvasculature integrity in the brain, which may prove beneficial to cognition while allowing for better tumor control in the clinic.

INTRODUCTION

Radiotherapy is a frontline treatment for nearly all malignancies of the central nervous system (CNS) (1, 2), and is frequently used to eradicate certain vascular abnormalities such as arteriovenous malformations (AVM) (3). While prescribed doses for the management of glioma, medulloblastoma and AVM vary, in nearly every instance such treatments elevate the risk of stroke. The link between cancer and cerebrovascular disease has been reviewed (4, 5), and in the case of radiotherapy the risk of stroke is nearly doubled (6). This is a particular concern for survivors of medulloblastoma (7, 8), who are also prone to cerebral microbleeds (9) and vascular changes including vasculopathy resulting from their intensive cranio-spinal irradiation regimen using photons or protons (10, 11). Higher-dose (up to 25 Gy) gamma knife/stereotactic approaches for the treatment of vascular malformations also elevates the chance of hemorrhage, pointing to the longer-term risks of targeted non-cancer therapies in the brain (3, 12–14).

A direct link between radiation-induced vascular damage and neurocognitive dysfunction remains to be completely elucidated, confounded by the fact that each of these normal tissue complications exhibits different dose response and temporal relationships (15). Neurocognitive dysfunction can manifest after single-fraction irradiation in the dose range of 10 Gy, and in the relative absence of structural changes indicative of edema, typically requiring total fractionated doses in excess of 40 Gy for visualization by magnetic resonance (MR) and diffusion tensor (DT) imaging (16). Regardless of the mechanistic link, it is apparent that radiation-induced normal tissue injury involves both stromal and parenchymal compartments of the brain, and includes a variety of changes that can manifest and persist long after the cessation of treatments. In this light, the ultra-high-dose-rate radiotherapy known as FLASH has generated considerable interest due to its marked capability to minimize normal tissue complications in a variety of organs using multiple pre-clinical models and, at least up to now, without compromising tumor control (17, 18). In the brain, FLASH has been shown to spare a variety of neurocognitive indices, preserve host neuronal structure and attenuate neuro-inflammation, evidenced by reductions in astrogliosis and microgliosis (19). Despite the documented benefits of FLASH in studies using fish, rodents, cats and mini-pigs (17, 19–22), details regarding the effect of this novel radiation modality on vascular end points remain relatively unknown. Previously published work analyzing the pulmonary vasculature has demonstrated the capability of FLASH to reduce damage by preventing the activation of apoptotic cascades caused by conventional-dose-rate radiation (23). However, whether the benefits of FLASH extend to the complex blood-brain barrier, responsible in part for maintaining CNS integrity, has remained unknown, providing the impetus for the current work.

Previously published work by our group has provided significant data demonstrating the neuroprotective effects of FLASH and defining the critical physical parameters required (19–21). Specifically, previously published studies in mice have defined dose-rate cutoffs for neurocognitive sparing after acute (≤10 Gy), whole-brain irradiation (21). Related work has found that neuroprotective benefits resulting from FLASH when compared to conventional-dose-rate irradiation (CONV) extend from early (one month) to later (six months) postirradiation times (19). In the current work, we evaluated the response of the vasculature in the brain to both radiation modalities at early times (24 h and one week) and to a relatively higher single dose (25 Gy, whole-brain irradiation) in an effort to approximate the radiotherapeutic management of certain vascular abnormalities. In addition, we analyzed vascular changes in the CNS at a later time (one month), using a single fraction (10 Gy, whole-brain irradiation) known to compromise long-term cognition. Here we report on some of the first evidence that FLASH provides significant protection to the CNS vasculature when compared against isodoses delivered at conventional dose rates.

MATERIALS AND METHODS

Animals

All animal procedures were conducted in accordance to and Swiss ethics committee (VD3241) and the University of California, Irvine Institutional Animal Care and Use Committee (IACUC) for animal experimentation. Eight-week-old female C57Bl/6J mice were purchased from Charles River Laboratories (France) and aged until 10 weeks when they were irradiated.

Irradiations

Single-fraction, whole-brain irradiations were performed on a prototype Oriatron 6e, 6-MeV electron beam linear accelerator (LINAC) at the Lausanne University Hospital (Lausanne, Switzerland), as described elsewhere (24). Dosimetry has been extensively described and published to ensure reproducible reliable delivery (24–27). For short-term studies, animals received a head-only, single dose of 25 Gy using a 17-mm graphite applicator at either CONV dose rate(0.09 Gy/s) or ultra-high-dose-rate FLASH (FLASH, instantaneous intra-pulse dose rate, $6.9 \cdot 10^6$ Gy/s at a mean dose rate of 2,500 Gy/s) (Table 1). These animals were euthanized 24 h (n = 12 per group) or one week (n = 12 per group) postirradiation and 30 min after lectin injection. To study long-term vascular toxicity, a second cohort of animals (n = 12 per group) received 10 Gy of the previously described CONV or FLASH (delivered at $5.6 \cdot 10^6$ Gy/s in a single 1.8 μs pulse) (Table 1). These animals were euthanized one month postirradiation and 30 min after tomato lectin injection.

Lectin Injection and Perfusions

To accurately image microvasculature of the brain, one half of all treatment groups were injected with tomato lectin (Vector® Laboratories, Burlingame, CA) 30 min prior to sacrifice. Lectin, 100 μg (1 μg/1 μl saline), was delivered via retro-orbital i.v. injection (Dylight® 488 Tomato Lectin; Vector Laboratories) using a 32g syringe. Animals were then intracardially perfused using 25 ml of heparinized saline, followed immediately by 75 ml of 4% paraformaldehyde (PFA) using a Peri-Stare™ Pro peristaltic pump (World Precision

Instruments, Sarasota, FL) delivered at 16 ml/min. Brain tissue was extracted and allowed to fix overnight in 4% PFA at 4°C before being transferred to phosphate buffered saline (PBS) with 0.01% NaN_3 for transportation and storage. Tissue later underwent a sucrose gradient (10%, 20%, 30% per volume) and OCT (Surgipath® FSC 22® Clear; Leica Microsystems, Wetzlar, Germany) embedded before being coronally sectioned at 30 μm using a cryostat, and then stored in PBS with 0.01% NaN_3 at 4°C for later analysis.

Immunohistochemistry and Image Collection

Tight junction markers and eNOS.—Two sections per brain were selected from the ventral hippocampus approximately 300 μm apart. Immunofluorescence to detect the expression of claudin-5 (CLDN5), occludin (OCLN) and endothelial nitric oxide synthase (eNOS) was performed on lectin-injected tissues. Brain sections were initially washed and permeabilized with PBS and Triton™ (0.1%) and blocking was performed in 10% goat serum, 0.2% bovine serum albumin (BSA) and 0.1% Tween®. Brain sections were incubated overnight at 4°C in 3% goat serum, 0.1% BSA and 0.1% Tween with the primary antibodies against CLDN5 (Rabbit anti-CLDN5 1:200), OCLN (Mouse anti-OCLN, 1:250) and eNOS (Rabbit anti-eNOS 1:250), all from Invitrogen™ (Carlsbad, CA). The next day, tissues were incubated for 1 h at room temperature with the following secondary antibodies: Goat anti-Mouse 647 (1:500) and Goat anti-Rabbit 594 (1:400), both from Abcam ® (Cambridge, MA) and Goat anti-Rabbit 647 (1:400; Thermo Fisher Scientific™ Inc., Waltham, MA), before counterstaining with DAPI. Tissues were then slide mounted and imaged at 40× using a Nikon Eclipse Ti-E Confocal (Tokyo, Japan) or Olympus® FV3000 Confocal (Tokyo, Japan) at 40×.

Volumetric analysis.—Four hippocampal sections were selected from each lectin-perfused brain ~300 μm apart, mounted to slides and imaged at 20×. Images were taken along the stratum radiatum and the molecular layer. This region was chosen due to its high level of vascularization and relationship to cognitive effects. Z-stack images were taken at 20 μm thickness and then processed using Imaris 3D rendering software (Bitplane AG, Zurich, Switzerland) as described elsewhere (28).

Imaris 3D Rendering.—All Z-stack images were imported into Imaris version 9.3.1 and deconvoluted using an adaptive, theoretical PSF batch processing. Deconvoluted images were then processed for 3D surface analysis for lectin, OCLN and CLDN5, while a spot analysis was performed for eNOS. When analyzing for tight junction markers, volumes of lectin and either OCLN or CLDN5 were colocalized and recorded. To evaluate the cellular regulation of the microvasculature, eNOS measurements were quantified based on the volume of any spot within 5 μm of 3D-rendered lectin. This allowed for removal of eNOS expression from other cell types not associated with the microvasculature.

Apoptosis.—Interrogation of apoptosis was performed on two sections per region, the subventricular zone (SVZ) and dentate gyrus (DG), per animal (n = 4), 24 h postirradiation. A TUNEL assay kit was used (ApopTag® In Situ Apoptosis Detection Kit; Sigma-Aldrich® LLC, St. Louis, MO) to quantify the number of Tdt^+ cells that colocalized with $DAPI^+$

nuclei in either the SVZ or DG. Imaris software allowed for quantification of $DAPI^+$ cells, while Tdt^+ cells were scored blind by hand.

RESULTS

FLASH does not Induce Vasogenic Edema or eNOS in the Microvasculature

Previously published work has shown that CONV dose-rate irradiation influences overall blood vessel volume (28). To determine the potential effects of FLASH on the vascular compartment, irradiated animals were injected with lectin and blood vessel volume was measured. Representative images of the Imaris 3D rendering of lectin are shown (Fig. 1A). The data revealed no significant changes at 24 h [$F_{(2,43)} = 0.7725$, $P = 0.4682$] (Fig. 1B), however, a significant group effect was found at one week postirradiation [$F_{(2,45)} = 8.059$, P 0.001] (Fig. 1C). A significant increase in total blood vessel volume was observed after CONV compared to controls ($P \leq 0.01$), whereas no modifications in volume were observed after FLASH one week after 25 Gy irradiation.

Expression of eNOS has been demonstrated to induce vasogenic dilation and/or edema by production of NO (29, 30). To investigate the contribution of eNOS to the vasogenic edema, shown in Fig. 1, we measured eNOS production in the molecular layer and stratum radiatum within the hippocampus (Fig. 2). Representative images show eNOS expression throughout these regions of the hippocampus (Fig. 2A). Consistent with previous observations reported elsewhere, eNOS was also expressed within the DG, pyramidal cells and astrocytes (31–33). eNOS was found to be expressed in cells lining the lectin-stained lumen of the microvasculature. Therefore eNOS expression was quantified within the nearby vicinity of lectin-stained vessels to focus on proximal “paracrine” cellular regulation. This allowed for quantification of protein levels within support cells of the microvasculature. No change in eNOS immunoreactivity was observed at 24 h postirradiation in either the CONV or FLASH group (Fig. 2B). Nevertheless, a significant group effect was observed at one week postirradiation [$F_{(2,31)} = 5.753$, $P = 0.0075$] (Fig. 2C). CONV induced increased eNOS immunoreactivity when compared to controls and FLASH ($P \leq 0.05$).

FLASH does not Induce Tight Junction Protein Degeneration

Previous studies designed to interrogate the blood-brain barrier, CLDN5 and OCLN were utilized as markers of the efficacy of epithelial cell adhesion (34, 35). To determine the effect of CONV and FLASH on the integrity of the blood-brain barrier, measurements of tight junction proteins colocalized with $lectin^+$ blood vessels were performed. Representative images of microvasculature and tight junction colocalization are shown in Fig. 3A. No significant modifications in OCLN expression were observed 24 h postirradiation (Fig 3B). However, analysis of OCLN/lectin colocalization at one week postirradiation showed a significant group effect within the hippocampus [$F_{(2,31)} = 12.12$, $P < 0.0001$] (Fig. 3B) and the SVZ [$F_{2,31)} = 11.92$, $P = 0.0002$] (Fig. 3B). Multiple comparisons analysis indicated a significant drop in OCLN expression after CONV in both subregions ($P < 0.05$ and $P <$ 0.001, hippocampus and SVZ, respectively), whereas OCLN expression was preserved in FLASH-irradiated brains. A significant group effect for CLDN5 immunoreactivity was observed 24 h after 25 Gy irradiation within the hippocampus [$F_{(2,29)} = 7.219$, $P = 0.0029$]

(Fig. 3C). Multiple comparisons test showed an increased level of CLDN5 colocalized to lectin in the hippocampus after FLASH compared to control ($P \leq 0.05$) and CONV ($P \leq 0.01$) groups. Within the SVZ, 25 Gy at either dose rate failed to induce any significant changes in the CLDN5 immunoreactivity (Fig 3C). However, by one week postirradiation, significant group effects were found within the hippocampus [$F_{(2,30)} = 13.43$, $P < 0.0001$] (Fig. 3C) and the SVZ [$F_{(2,29)} = 5.418$, $P = 0.01$] (Fig. 3C). Within the hippocampus, a significant drop in CLDN5 expression colocalized with lectin was observed after CONV when compared to controls ($P \leq 0.001$) and FLASH ($P \leq 0.01$). No change was observed after FLASH compared to control. Within the SVZ, CLDN5 expression in the CONV group was reduced compared to controls ($P \leq 0.01$). Altogether, these results suggest that FLASH does not induce blood-brain barrier alteration characterized by a decreased expression of tight junction proteins described after CONV at early and late timepoints postirradiation.

FLASH Induces Less Apoptosis in the Normal Brain after 25 Gy

To determine if FLASH protected neurogenic regions (SVZ, DG) of the brain from early apoptosis, a TUNEL assay was performed 24 h postirradiation (Fig. 4). Figure 4A shows representative images of the SVZ (left-side column) and DG (right-side column). The data revealed a significant group effect in both the SVZ [$F_{(2,32)} = 32.36$, $P < 0.0001$) (Fig. 4B) and DG regions [$F_{(2,28)} = 22.38$, $P < 0.0001$] (Fig. 4C). Within the SVZ, a marked increase in Tdt^+ cells was observed after CONV compared to controls ($P < 0.0001$) and FLASH ($P \leq 0.05$). Increased levels of Tdt^+ cells were also observed in the FLASH group compared to the controls ($P \leq 0.001$), but were significantly lower than observed after CONV ($P < 0.05$). Similar results were found in the hippocampal DG. CONV induced increased yields of Tdt^+ cells compared to controls ($P < 0.0001$) and FLASH ($P \leq 0.01$). Differences in the number of Tdt^+ cells between control and FLASH cohorts were not statistically significant. These results indicate that FLASH induced less apoptosis than CONV irradiation in the neurogenic regions of the brain.

FLASH Protects the Microvasculature from Radiation-Induced Deficits One Month after Irradiation

To determine if a dose known to induce cognitive deficits (10 Gy) affects the microvasculature, measurements of vascular volume and eNOS vascular dilation were analyzed at one month postirradiation. A significant group effect was found when total lectin volume was analyzed [$F_{(2,44)} = 11.91$, $P < 0.0001$] (Fig. 5A). A significant increase in lectin volume was observed after CONV irradiation compared to controls ($P \leq 0.001$) and FLASH ($P < 0.05$) (Fig. 5A). While an increase in average lectin volume was measured for FLASH compared to controls ($P = 0.075$), no statistically significant change was found (Fig. 5A). eNOS colocalization was measured to determine if levels coincided with this increased vascular volume. Changes in the level of eNOS expression colocalized with the vasculature one month postirradiation were found to have a significant group effect [$F_{(2,32)} = 5.075$, $P = 0.0122$) (Fig. 5B). Expression of eNOS in the hippocampus after CONV irradiation was elevated significantly compared to control ($P \leq 0.05$) and FLASH ($P \leq 0.05$) groups; however, no significant change between control and FLASH was observed.

Vascular integrity was also interrogated at one month (10 Gy) by measuring levels of tight junction proteins that colocalized with lectin. Analysis of OCLN-lectin immunoreactivity indicated a significant group effect within the hippocampus [$F_{(2,33)} = 4.922$, $P = 0.0139$]. Multiple comparison analysis revealed that control animals exhibited higher levels of OCLN-lectin colocalization compared to CONV irradiation ($P \leq 0.05$) and FLASH ($P \leq 0.05$) (Fig. 6A) groups. Within the SVZ, similar albeit non-significant trends were observed.

Analysis of CLDN5-lectin immunoreactivity within the hippocampus uncovered a significant group effect [$F_{(2,30)} = 4.288$, $P = 0.0230$], but not in the SVZ [$F_{(2,27)} = 2.226$, $P = 0.1274$] (Fig. 6B). Compared to controls, FLASH exhibited no statistically significant difference of CLDN5-lectin colocalization in the hippocampus; however, significant decreases were found in CONV-irradiated cohorts ($P \leq 0.05$). Within the SVZ, CLDN5-lectin staining was increased significantly after FLASH compared to controls ($P \leq 0.05$) and CONV ($P \leq 0.01$). Decreased immunoreactivity of CLDN5 compared to controls was non-significant. Collectively, these data indicate that FLASH protects against vascular dilation while providing some protection to markers of tight junctions, one month after irradiation.

DISCUSSION

In the current study, we have shown that FLASH can circumvent some of the early and more persistent detrimental effects to the CNS microvasculature compared to CONV. At acute timepoints, we showed that 25 Gy FLASH did not modify key vascular parameters including blood vessel volume or the expression of eNOS and tight junction proteins and did not induce apoptosis, while 25 Gy CONV irradiation altered the brain microvasculature. Interestingly after 10 Gy FLASH, the majority of these vascular parameters remained at normal levels at a later timepoint as well.

In this study, we investigated the effect of high-dose radiation on the brain as treatment for vascular abnormalities in humans using gamma knife doses of approximately 25 Gy, which is highly focused onto small volumes. In our experiments, we had no access to conformal irradiation and used whole-brain irradiation. In this context, 25 Gy delivered in a single fraction would be lethal, especially after CONV. Therefore, to make vascular analyses feasible, animals were sampled at earlier postirradiation times. While in one published study, the CNS benefits one month after 30 Gy whole-brain FLASH have been reported (36), we opted to focus our study of 25 Gy on the earlier postirradiation times of 24 h and one week to ensure survival. Then, the protracted timepoint was studied using 10 Gy whole-brain irradiation, a dose known to differentially affect neurocognitive outcomes in mice subjected to either irradiation modality.

Higher doses of cranial irradiation have been shown to temporarily induce microvasculature damage, which is part of the initial radiation-induced pathogenic signals (37, 38). Initial morphologic alterations of the microvasculature have also been implicated in the progression of white matter necrosis likely caused by decreased metabolism stemming from reduced oxygen transfer (15, 39). In the current study, microvasculature morphology was analyzed using lectin, since its capability to efficiently stain blood vessels has been found to be more accurate than the use of endothelial antibodies (40). An analysis of the microvasculature

indicated that CONV induced a significant increase in vessel volume associated with production of the vasodilator eNOS (41) at one week after 25 Gy irradiation. This effect was not observed after FLASH. Interestingly, previously published studies from our group have shown that FLASH produced a lower level of reactive oxygen species (19) which may explain the decreased levels of eNOS reported in the current work. However, additional mechanisms can be involved. It has been reported that HSP90 and ATM phosphorylation induced during DNA repair were responsible for activation of eNOS (30), suggesting that the attenuation of DNA damage after FLASH, as recently reported by Fouillade *et al.* (42), could restrain eNOS expression and help maintain a normal vascular morphology. While further studies at additional postirradiation times are clearly needed to expand our findings, the current data point to the capability of FLASH to attenuate early changes in vessel volume.

Expression of tight junction proteins have been known to coincide with the overall integrity and permeability of the blood-brain barrier (34, 37). We found that FLASH preserved the integrity of the blood-brain barrier when compared to CONV irradiation. Using markers for CLDN5 and OCLN, a stark difference between FLASH and CONV one week postirradiation was observed. Interestingly, FLASH caused a significant increase in CLDN5 and an upward trend in OCLN 24 h compared to CONV and control in the hippocampus, postirradiation. While further work is required to elucidate the molecular basis of this transient increase (transcriptional, post-translational, reduced turnover, etc.) FLASH is clearly engaging different signaling pathways in the irradiated brain. Previously reported work has shown that breakdown of CLDN5 and OCLN is directly related to an inflammatory response involving VEGF (43), suggesting that the observed attenuation of neuroinflammation after FLASH (19, 21) may contribute to the preservation of tight junctions.

The capability of FLASH to reduce ROS production may well account for the observed reduction in apoptotic cells in the neurogenic regions of the SVZ and the DG, but disruptions in the microvasculature and subsequent microenvironmental factors could also contribute to cell death. Previously published studies have shown that proliferating neural precursor cells cluster around small vessels, suggesting that even small disruptions in homeostasis could negatively affect neurogenesis by altering cell survival and/or later recruitment of neural precursor cells (44). It has also been shown that radiation-induced microvasculature changes could alter neurogenesis through changes in the microenvironment (45). These data suggest that damage to the microvasculature could have persistent adverse effects on the regenerative reserve of the brain, an effect that FLASH was able to circumvent, possibly through the preservation of vascular integrity.

Late occurring damage to the brain after radiotherapy is a significant concern for thousands of people who are treated for CNS malignancies each year. To address the potential longer-term cerebrovascular benefits of FLASH, irradiated brains were analyzed after a dose (10 Gy) and at a time (one month) known to coincide with neurocognitive decline. Analogous measurements conducted on the microvasculature under these conditions indicated that FLASH was able to significantly attenuate the increased vessel volume and elevated eNOS expression found after CONV. While the differences in the expression of tight junction

proteins at this dose and time were less pronounced between the irradiation modalities, FLASH was able to maintain CLDN5 expression in the SVZ. For survivors of brain tumors, alterations to microvasculature integrity can lead to debilitating effects that can develop months to years after treatment, manifesting as white matter necrosis and/or edema (46). Although the exact mechanism of delayed CNS radiation injury is not fully understood, the vascular injury hypothesis attributes many of these detrimental effects to vascular dilation, vascular wall thickening, endothelial cell nuclear enlargement and breakdown of tight junctions (47). While results from this study indicate that FLASH may reduce some of the potential underlying causes of clinically relevant vascular side effects, further work will be needed to more conclusively link the underlying causes affecting cerebrovascular and neurocognitive outcomes in the irradiated brain.

This study serves to build on the growing body of knowledge supporting the “FLASH effect”, operationally defined as the capability of FLASH to spare normal tissue toxicities. Results from this study corroborate many previously published findings demonstrating that normal tissue damage is reduced within the brain and other tissues receiving FLASH compared to CONV (19, 21, 23). In addition, other CNS complications such as white matter necrosis (48), hearing loss (7) and vascular abnormalities resulting from larger-field or targeted high-dose approaches for treating AVM (3, 13, 14, 49) may also benefit from FLASH. As early studies identified the dose rate as the essential parameter (21, 23), more recently published work emphasizes that additional physics parameters such as the instantaneous dose rate, pulse frequency and pulse duration, are critical to achieve the FLASH effect (19, 50, 51). Here, using maximal electron current to produce the highest instantaneous dose rate possible with the eRT6 (Table 1), investigations of the FLASH effect have been extended to the normal vasculature of the irradiated brain. While further work is required to substantiate the potential vascular benefits in the CNS over a larger range of doses and postirradiation times, our study demonstrates the beneficial effect of FLASH compared to CONV radiation on important cerebrovascular end points. The inclusion of additional functional studies coupled with dose fractionation to more thoroughly evaluate whether FLASH might mitigate cerebral bleeds, stroke and white matter necrosis would also add important insights. Nonetheless, the current findings have important repercussions for anyone subjected to cranial radiotherapy, and in particular for survivors of pediatric brain malignancies, where FLASH provides a potentially new approach for mitigating additional cerebrovascular complications, the risks of which have been clearly shown to increase with age (7).

ACKNOWLEDGMENTS

This study was supported by grants from the ISREC Foundation. We thank Biltema for their donation (to MCV). Further support was provided by Synergia (FNS CRS II5_186369 to MCV), the National Institutes of Health (NIH grant no. P01CA244091 to MCV and CLL) and the National Institute of Neurological Disorders and Stroke (NINDS grant no. NS089575 to CLL). PMG was supported by Ecole Normale Supérieure de Cachan fellowship (MESR), FNS No. 31003A_156892 and the ISREC Foundation. We also thank the Animal Facilities of Epalinges for the animal husbandry.

REFERENCES

1. Butler JM, Rapp SR, Shaw EG. Managing the cognitive effects of brain tumor radiation therapy. Curr Treat Options Oncol 2006; 7:517–23. [PubMed: 17032563]
2. Butler RW, Fairclough DL, Katz ER, Kazak AE, Noll RB, Thompson RD, et al. Intellectual functioning and multi-dimensional attentional processes in long-term survivors of a central nervous system related pediatric malignancy. Life Sci 2013; 93:611–6. [PubMed: 23727455]
3. Seymour ZA, Chan JW, Sneed PK, Kano H, Lehocky CA, Jacobs RC, et al. Dose response and architecture in volume staged radiosurgery for large arteriovenous malformations: A multi-institutional study. Radiother Oncol 2019; 144:180–8. [PubMed: 31835173]
4. Adams HP Jr. Cancer and cerebrovascular disease. Curr Neurol Neurosci Rep 2019; 19:73. [PubMed: 31440841]
5. Zaorsky NG, Zhang Y, Tchelebi LT, Mackley HB, Chinchilli VM, Zacharia BE. Stroke among cancer patients. Nat Commun 2019; 10:5172. [PubMed: 31729378]
6. Huang R, Zhou Y, Hu S, Ren G, Cui F, Zhou PK. Radiotherapy exposure in cancer patients and subsequent risk of stroke: A systematic review and meta-analysis. Front Neurol 2019; 10:233. [PubMed: 30930843]
7. King AA, Seidel K, Di C, Leisenring WM, Perkins SM, Krull KR, et al. Long-term neurologic health and psychosocial function of adult survivors of childhood medulloblastoma/PNET: a report from the Childhood Cancer Survivor Study. Neurooncol 2017; 19, 689–98.
8. Wells EM, Ullrich NJ, Seidel K, Leisenring W, Sklar CA, Armstrong GT, et al. Longitudinal assessment of late-onset neurologic conditions in survivors of childhood central nervous system tumors: a Childhood Cancer Survivor Study report. Neurooncol 2018; 20:132–42.
9. Roongpiboonsopit D, Kuijf HJ, Charidimou A, Xiong L, Vashkevich A, Martinez-Ramirez S, et al. Evolution of cerebral microbleeds after cranial irradiation in medulloblastoma patients. Neurology 2017; 88:789–96. [PubMed: 28122904]
10. Hersh DS, Moore K, Nguyen V, Elijovich L, Choudhri AF, Lee-Diaz JA, et al. Evaluation and treatment of children with radiation-induced cerebral vasculopathy. J Neurosurg Pediatr 2019; Epub ahead of print.
11. Tanyildizi Y, Keweloh S, Neu MA, Russo A, Wingerter A, Weyer-Elberich V, et al. Radiation-induced vascular changes in the intracranial irradiation field in medulloblastoma survivors: An MRI study. Radiother Oncol 2019; 136:50–5. [PubMed: 31015129]
12. Gauden AJ, McRobb LS, Lee VS, Subramanian S, Moutrie V, Zhao Z, et al. Occlusion of animal model arteriovenous malformations using vascular targeting. Transl Stroke Res 2020; 11:689–699.
13. Hasegawa H, Yamamoto M, Shin M, Barfod BE. Gamma knife radiosurgery for brain vascular malformations: Current evidence and future tasks. Ther Clin Risk Manag 2019; 15:1351–67. [PubMed: 31819462]
14. Starke RM, McCarthy DJ, Chen CJ, Kano H, McShane BJ, Lee J, et al. Hemorrhage risk of cerebral dural arteriovenous fistulas following Gamma Knife radiosurgery in a multicenter international consortium. J Neurosurg 2019; (10.3171/2018.12.JNS182208).
15. Tofilon PJ, Fike JR. The radioresponse of the central nervous system: a dynamic process. Radiat Res 2000; 153:357–70. [PubMed: 10798963]
16. Makale MT, McDonald CR, Hattangadi-Gluth JA, Kesari S. Mechanisms of radiotherapy-associated cognitive disability in patients with brain tumours. Nat Rev Neurol 2017; 13:52–64. [PubMed: 27982041]
17. Montay-Gruel P, Meziani L, Yakkala C, Vozenin MC. Expanding the therapeutic index of radiation therapy by normal tissue protection. Br J Radiol 2019; 92:20180008. [PubMed: 29694234]
18. Vozenin MC, Hendry JH, Limoli CL. Biological benefits of ultra-high dose rate FLASH radiotherapy: Sleeping beauty awoken. Clin Oncol (R Coll Radiol) 2019; 31:407–15. [PubMed: 31010708]
19. Montay-Gruel P, Acharya MM, Petersson K, Alikhani L, Yakkala C, Allen BD, et al. Long-term neurocognitive benefits of FLASH radiotherapy driven by reduced reactive oxygen species. Proc Natl Acad Sci U S A 2019; 116:10943–51. [PubMed: 31097580]

20. Montay-Gruel P, Bouchet A, Jaccard M, Patin D, Serduc R, Aim W, et al. X-rays can trigger the FLASH effect: Ultrahigh dose-rate synchrotron light source prevents normal brain injury after whole brain irradiation in mice. Radiother Oncol 2018; 129:582–8. [PubMed: 30177374]
21. Montay-Gruel P, Petersson K, Jaccard M, Boivin G, Germond JF, Petit B, et al. Irradiation in a flash: Unique sparing of memory in mice after whole brain irradiation with dose rates above 100Gy/s. Radiother Oncol 2017; 124:365–9. [PubMed: 28545957]
22. Vozenin MC, De Fornel P, Petersson K, Favaudon V, Jaccard M, Germond JF, et al. The advantage of FLASH radiotherapy confirmed in mini-pig and cat-cancer patients. Clin Cancer Res 2019; 25:35–42. [PubMed: 29875213]
23. Favaudon V, Caplier L, Monceau V, Pouzoulet F, Sayarath M, Fouillade C, et al. Ultrahigh dose-rate FLASH irradiation increases the differential response between normal and tumor tissue in mice. Sci Transl Med 2014; 6:245ra93.
24. Jaccard M, Duran MT, Petersson K, Germond JF, Liger P, Vozenin MC, et al. High dose-per-pulse electron beam dosimetry: Commissioning of the Oriatron eRT6 prototype linear accelerator for preclinical use. Med Phys 2018; 45:863–74. [PubMed: 29206287]
25. Jaccard M, Petersson K, Buchillier T, Germond JF, Duran MT, Vozenin MC, et al. High dose-per-pulse electron beam dosimetry: Usability and dose-rate independence of EBT3 Gafchromic films. Med Phys 2017; 44:725–35. [PubMed: 28019660]
26. Petersson K, Jaccard M, Germond JF, Buchillier T, Bochud F, Bourhis J, et al. High dose-per-pulse electron beam dosimetry - A model to correct for the ion recombination in the Advanced Markus ionization chamber. Med Phys 2017; 44:1157–67. [PubMed: 28094853]
27. Jorge PG, Jaccard M, Petersson K, Gondre M, Duran MT, Desorgher L, et al. Dosimetric and preparation procedures for irradiating biological models with pulsed electron beam at ultrahigh dose-rate. Radiother Oncol 2019; 139:34–9. [PubMed: 31174897]
28. Craver BM, Acharya MM, Allen BD, Benke SN, Hultgren NW, Baulch JE, et al. 3D surface analysis of hippocampal microvasculature in the irradiated brain. Environ Mol Mutagen 2016; 57:341–9. [PubMed: 27175611]
29. Forstermann U, Sessa WC. Nitric oxide synthases: regulation and function. Eur Heart J 2012; 33:829–37, 837a–837d. [PubMed: 21890489]
30. Nagane M, Yasui H, Sakai Y, Yamamori T, Niwa K, Hattori Y, et al. Activation of eNOS in endothelial cells exposed to ionizing radiation involves components of the DNA damage response pathway. Biochem Biophys Res Commun 2015; 456:541–6. [PubMed: 25498542]
31. Iwase K, Miyanaka K, Shimizu A, Nagasaki A, Gotoh T, Mori M, et al. Induction of endothelial nitric-oxide synthase in rat brain astrocytes by systemic lipopolysaccharide treatment. J Biol Chem 2000; 275:11929–33. [PubMed: 10766821]
32. Lin LH, Taktakishvili O, Talman WT. Identification and localization of cell types that express endothelial and neuronal nitric oxide synthase in the rat nucleus tractus solitarii. Brain Res 2007; 1171:42–51. [PubMed: 17761150]
33. Michel T, Feron O. Nitric oxide synthases: which, where, how, and why? J Clin Invest 1997; 100:2146–52. [PubMed: 9410890]
34. Gunzel D, Yu AS. Claudins and the modulation of tight junction permeability. Physiol Rev 2013; 93:525–69. [PubMed: 23589827]
35. Paul D, Cowan AE, Ge S, Pachter JS. Novel 3D analysis of claudin-5 reveals significant endothelial heterogeneity among CNS microvessels. Microvasc Res 2013; 86:1–10. [PubMed: 23261753]
36. Simmons DA, Lartey FM, Schuler E, Rafat M, King G, Kim A, et al. Reduced cognitive deficits after FLASH irradiation of whole mouse brain are associated with less hippocampal dendritic spine loss and neuroinflammation. Radiother Oncol 2019; 139:4–10. [PubMed: 31253467]
37. Fauquette W, Amourette C, Dehouck MP, Diserbo M. Radiation-induced blood-brain barrier damages: An in vitro study. Brain Res 2012; 1433:114–26. [PubMed: 22153623]
38. Yuan H, Gaber MW, McColgan T, Naimark MD, Kiani MF, Merchant TE. Radiation-induced permeability and leukocyte adhesion in the rat blood-brain barrier: modulation with anti-ICAM-1 antibodies. Brain Res 2003; 969:59–69. [PubMed: 12676365]

39. Reinhold HS, Calvo W, Hopewell JW, van der Berg AP. Development of blood vessel-related radiation damage in the fimbria of the central nervous system. Int J Radiat Oncol Biol Phys 1990; 18:37–42. [PubMed: 2298633]
40. Iovino F, Orihuela CJ, Moorlag HE, Molema G, Bijlsma JJ. Interactions between blood-borne Streptococcus pneumoniae and the blood-brain barrier preceding meningitis. PLoS One 2013; 8:e68408. [PubMed: 23874613]
41. Heiss C, Rodriguez-Mateos A, Kelm M. Central role of eNOS in the maintenance of endothelial homeostasis. Antioxid Redox Signal 2015; 22:1230–42. [PubMed: 25330054]
42. Fouillade C, Curras-Alonso S, Giuranno L, Quelennec E, Heinrich S, Bonnet-Boissinot S, et al. FLASH irradiation spares lung progenitor cells and limits the incidence of radio-induced senescence. Clin Cancer Res 2020; 26:1497–506. [PubMed: 31796518]
43. Argaw AT, Asp L, Zhang J, Navrazhina K, Pham T, Mariani JN, et al. Astrocyte-derived VEGF-A drives blood-brain barrier disruption in CNS inflammatory disease. J Clin Invest 2012; 122:2454–68. [PubMed: 22653056]
44. Palmer TD, Willhoite AR, Gage FH. Vascular niche for adult hippocampal neurogenesis. J Comp Neurol 2000; 425:479–94. [PubMed: 10975875]
45. Monje ML, Mizumatsu S, Fike JR, Palmer TD. Irradiation induces neural precursor-cell dysfunction. Nat Med 2002; 8:955–62. [PubMed: 12161748]
46. Wiggermann V, Lapointe E, Litvin L, Graf C, Hernandez-Torres E, McKenzie M, et al. Longitudinal advanced MRI case report of white matter radiation necrosis. Ann Clin Transl Neurol 2019; 6:379–85. [PubMed: 30847370]
47. Kessler AT, Bhatt AA. Brain tumour post-treatment imaging and treatment-related complications. Insights Imaging 2018; 9:1057–75. [PubMed: 30411280]
48. Nagesh V, Tsien CI, Chenevert TL, Ross BD, Lawrence TS, Junick L, et al. Radiation-induced changes in normal-appearing white matter in patients with cerebral tumors: a diffusion tensor imaging study. Int J Radiat Oncol Biol Phys 2008; 70:1002–10. [PubMed: 18313524]
49. Seo YS, Ko IO, Park H, Jeong YJ, Park JA, Kim KS, et al. Radiation-induced changes in tumor vessels and microenvironment contribute to therapeutic resistance in glioblastoma. Front Oncol 2019; 9:1259. [PubMed: 31803626]
50. Bourhis J, Montay-Gruel P, Goncalves Jorge P, Bailat C, Petit B, Ollivier J, et al. Clinical translation of FLASH radiotherapy: Why and how? Radiother Oncol 2019; 139:11–17. [PubMed: 31253466]
51. Wilson JD, Hammond EM, Higgins GS, Petersson K. Ultra-high dose rate (FLASH) radiotherapy: Silver bullet or fool's gold? Front Oncol 2019; 9:1563. [PubMed: 32010633]

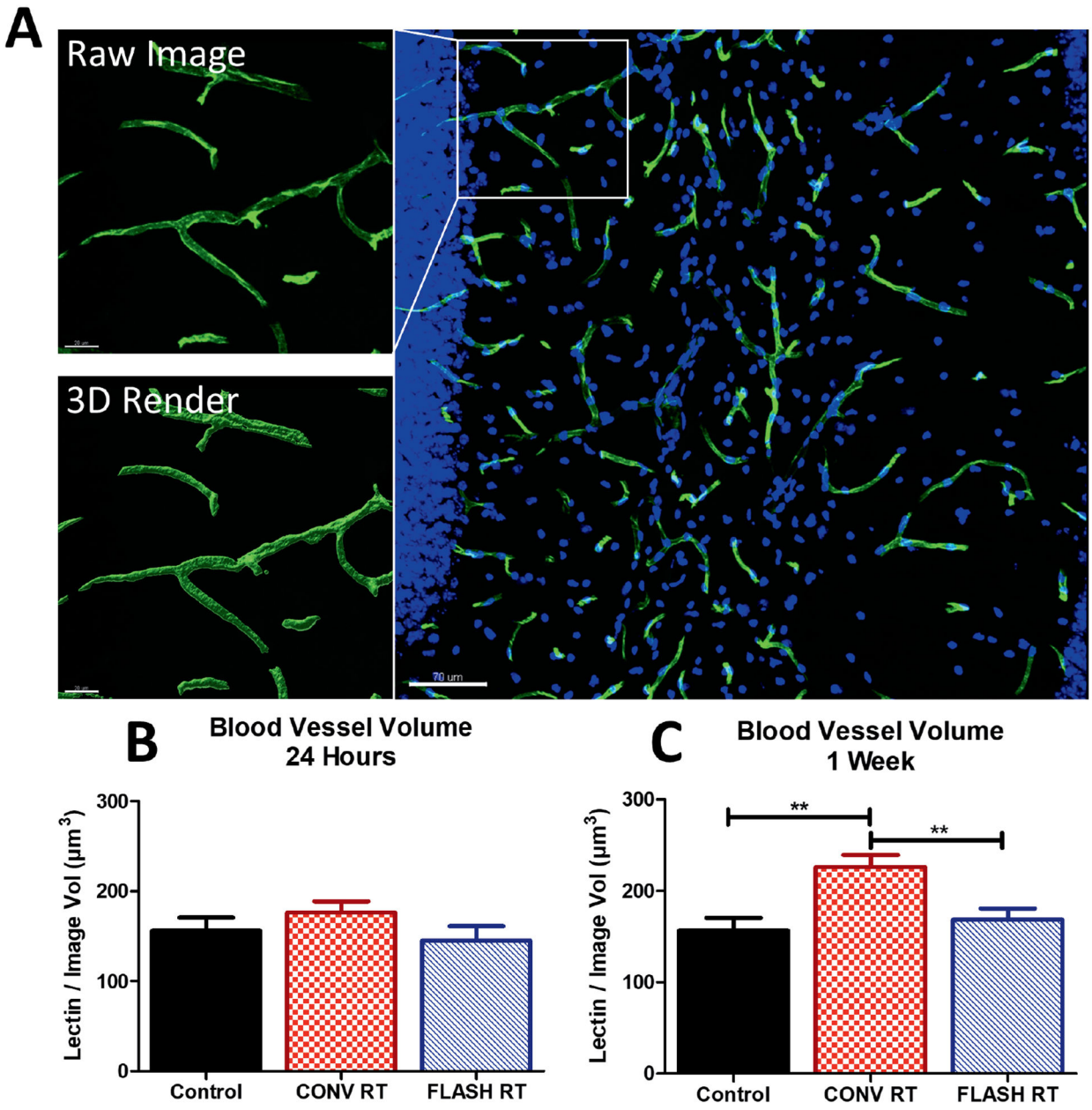

FIG. 1.

FLASH does not induce vascular dilation within the brain microvasculature. Animals were injected with tomato lectin 30 min prior to sacrifice and volumetric analysis was performed. Panel A: Representative images of lectin volume quantification at one week postirradiation. Scale bars = 20 and 70 μm. Panels B and C: Quantification of lectin volume at 24 h and one week after 25 Gy irradiation. CONV increased the total volume of lectin at one week when compared to control and FLASH. Data shown are the mean ± SEM (n = 4 per group, four images analyzed per animal). $*P < 0.05$, $**P \leq 0.01$ (ANOVA with Bonferroni's multiple comparisons test).

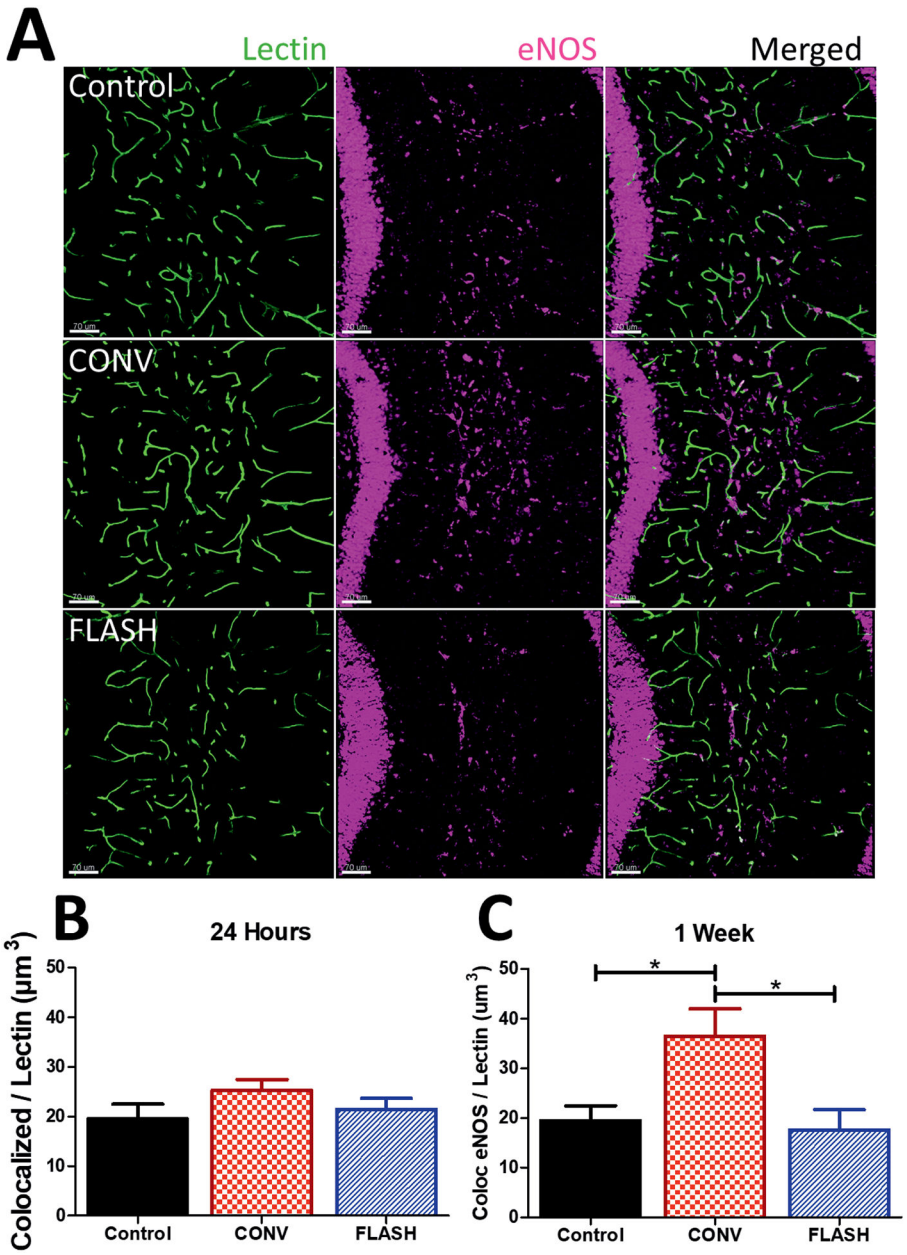

FIG. 2.

FLASH did not elevate vascular eNOS in the brain. Volumetric analysis of eNOS colocalized with lectin was performed. Panel A: Representative images of eNOS immunoreactivity were converted to 3-D renderings using Imaris at one week postirradiation. Scale bars = 70 µm. Panels B and C: Quantitative analysis of eNOS colocalized within 5 µm of lectin-stained microvasculature at 24 h and one week. CONV increased levels of eNOS-lectin at one week compared to control and FLASH. Data shown are the mean ± SEM (n = per group, two images analyzed per animal). $*P < 0.05$ (ANOVA with Bonferroni's multiple comparisons test).

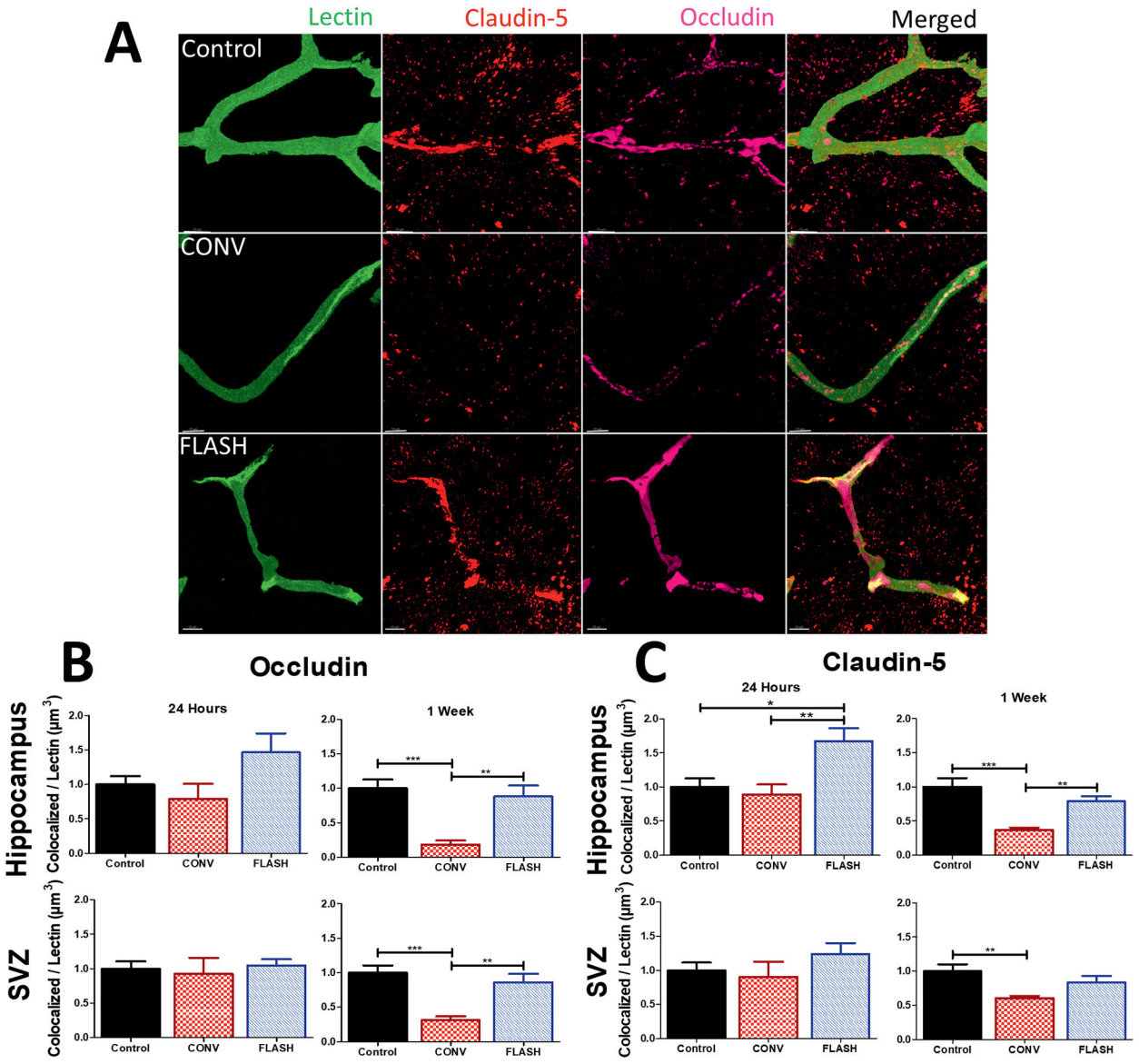

FIG. 3.

FLASH did not reduce immunoreactivity of CLDN5-lectin and OCLN-lectin as CONV irradiation did, at one week postirradiation. Volumetric analysis of markers CLDN5 and OCLN colocalized to lectin were quantified using Imaris software. Panel A: Representative images of CLDN5 and OCLN taken at the stratum radiatum of the hippocampus. Scale bars = 10 µm. Panels B and C: Analysis of OCLN and CLDN5 data at 24 h and one week within hippocampus and subventricular zone. CONV showed a significant drop-off of tight junction proteins at one week postirradiation compared to controls and FLASH. Data are the mean ± SEM (n = per group, two images analyzed per animal). $*P \leq 0.05$, $**P \leq 0.01$ and $***P \leq 0.001$ (ANOVA with Bonferroni's multiple comparisons test).

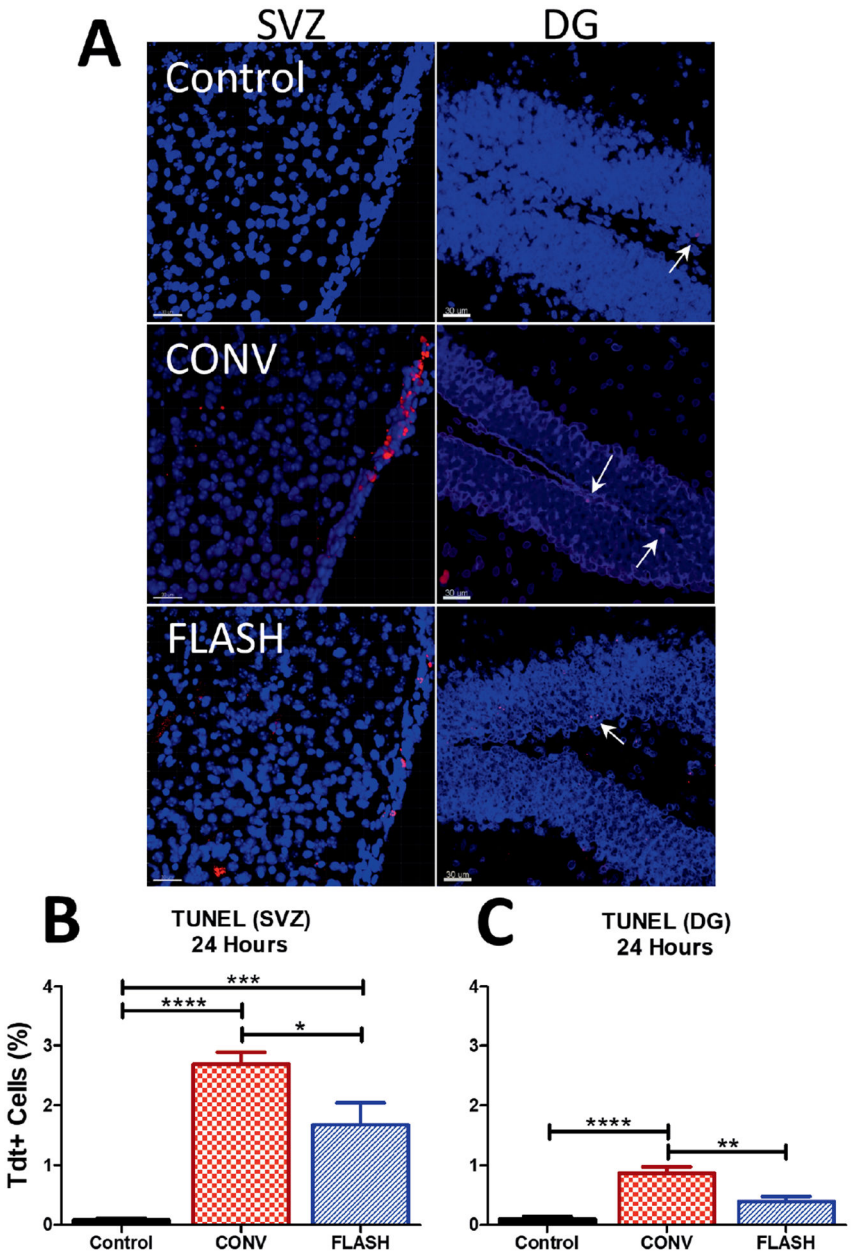

FIG. 4.

FLASH reduces apoptosis compared to CONV within neurogenic regions, 24 h postirradiation. TUNEL assay was performed to determine levels of apoptosis within the dentate gyrus (DG) and subventricular zone (SVZ). CONV-irradiated animals exhibited a significant increase when compared to FLASH and control in both the SVZ and DG. Representative images of Tdt^+ cells within the SVZ (left side) and DG (right side). Scale bars = 30 μm). Panels B and C: Analysis of Tdt^+ cells within the SVZ and DG at 24 h postirradiation. Data is shown as the mean ± SEM (n = 6 per group, two images analyzed per animal). $*P \leq 0.05$, $**P \leq 0.01$, $***P \leq 0.001$, $****P \leq 0.0001$ (ANOVA with Bonferroni's multiple comparisons test).

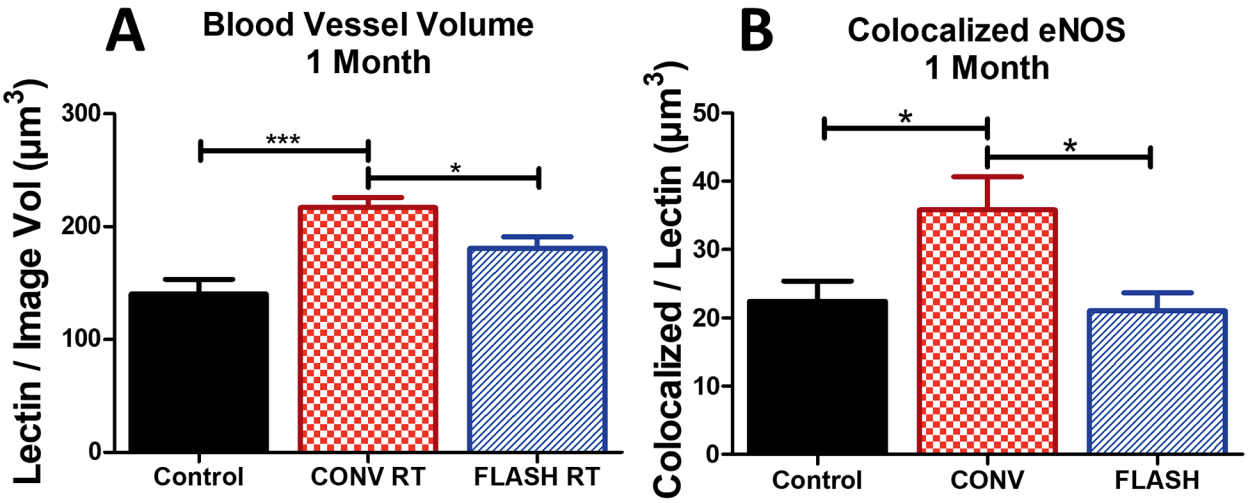

FIG. 5.

FLASH protects against eNOS-induced blood vessel dilation compared to CONV irradiation after one month (10 Gy) in the hippocampus. Animals were injected with tomato lectin 30 min prior to sacrifice and volumetric analysis was performed. Panel A: Quantification of lectin volume at one month postirradiation show that CONV dose rates cause an increase in lectin volume after 10 Gy that is not observed after FLASH ultra-high dose rates. Panel B: Colocalization of eNOS within 5 µm of lectin shows that FLASH does not induce an increase in immunoreactivity while CONV does. Blood vessel volume data shown are the mean ± SEM (n = 4 per group, four images analyzed per animal). eNOS data shown are the mean ± SEM (n = 6 per group, two images analyzed per animal). *$P \leq 0.05$, ***$P \leq 0.001$ (ANOVA with Bonferroni's multiple comparisons test).

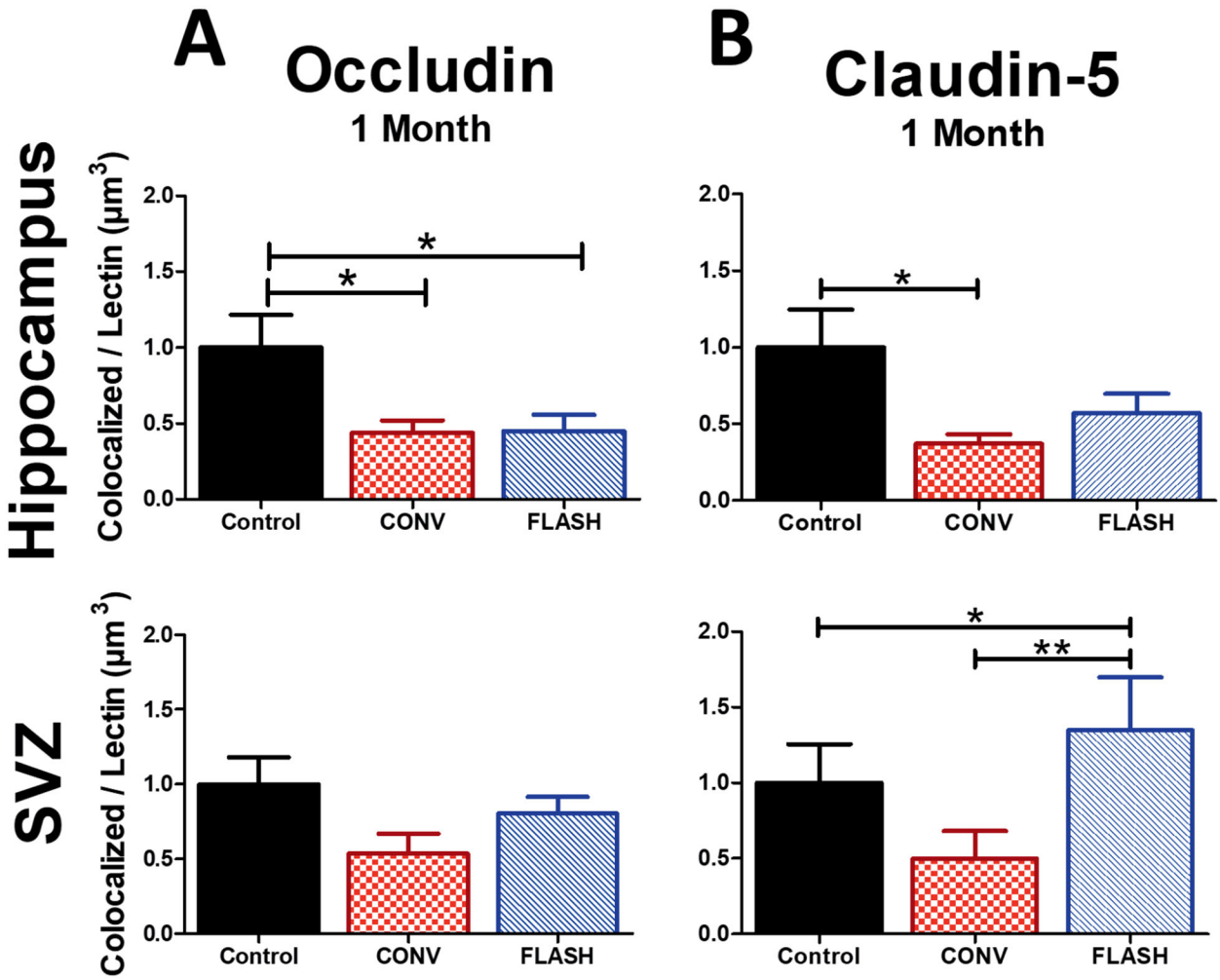

FIG. 6.

FLASH provides some protection against CONV irradiation-induced tight junction modification at one month after 10 Gy irradiation. Volumetric analysis of OCLN and CLDN5 colocalization with lectin were measured using Imaris software within the stratum radiatum of the hippocampus and SVZ. Panel A: Measurements of OCLN indicate that both FLASH and CONV decreased levels of immunoreactivity within the hippocampus, but did not significantly change levels within the SVZ compared to controls. Panel B: FLASH does not induce a significant decrease in CLDN5 that CONV dose rates do in the hippocampus. FLASH causes a significant increase of CLDN5 compared to both CONV and control. Data shown are the mean ± SEM (n = 6 per group, two images analyzed per animal). $*P \leq 0.05$, $**P \leq 0.01$ (ANOVA with Bonferroni's multiple comparisons test).

TABLE 1

Irradiation Parameters

	Prescribed dose			
	CONV		FLASH	
Beam parameters	**10 Gy**	**25 Gy**	**10 Gy**	**25 Gy**
Graphite applicator type and size (mm)	Circular Ø17	Circular Ø17	Circular Ø17	Circular Ø17
Source-to-surface distance (mm)	800	745	369–370	325
Pulse repetition frequency (Hz)	10	10	100	100
Pulse width (μs)	1.0	1.0	1.8	1.8
No. of pulses	1,170–1,180	2,620	1	2
Treatment time (s)	116.9–117.9	261.9	1.8×10^{-6}	1.0×10^{-2}
Mean dose rate (Gy/s)	0.09	0.1	5.6×10^{6}	2.5×10^{3}
Instantaneous dose rate (Gy/s)	8.5×10^{3}	9.5×10^{3}	5.6×10^{6}	6.9×10^{6}